Study on Characteristics of Weld Defect and Its Prevention in Electron Beam Welding (Report I)†
—Characteristics of Weld Porosities—

Yoshiaki ARATA*, Kiyoshi TERAI and Shozo MATSUDA****

Abstract

In this report it performed to investigate upon the types of representative macro weld defects (except crack) and also upon the characteristics of weld porosities which are produced in electron beam weld metal, using eight kinds of materials.

Moreover in these materials, six types of defects such as R-porosity, A-porosity, AR-porosity, unmelted lump, cold shut and spiking, is recognized. The occurring characteristics of these porosities is indicated positively by utilizing I_b-a_b coordinates.

It is proved to be closely related with R-porosity and spiking, with A-porosity and beam active parameter, a_b, and also with AR-porosity and arcing in electron gun.

Additional investigations are made on the effect of gases contained in the materials on the porosities.

1. Introduction

It is well known that the electron beam will be fairly utillized as an excellent heat source for welding.

The most important property of it is to produce an extreme weld deep penetration. It is, however, recognized that the proper defects of the electron beam weld tends to occur in the weld deep zone. Then it is necessary to study the occurring mechanism of these defects and to search its prevention due to extend the industrial application. So it was performed systematically.

So in this report, various investigations of the macroscopic defects such as porosity, unmelted lump, spiking, cold shut and so on except cracks, have been done systematically using eight kinds of metals such as ferrite steel, austenite steel, Aluminum, Titanium and so forth.

2. Experimental Procedure

2.1 Material Used

As shown in **Table 1,** eight kinds of metals were used in this experiments. These materials are three types of austenitic stainless steel of SUS27, SUS27N which contained 0.2 % N_2 and 30Cr—16NiN which contained 0.2% N_2 and higher percentage of Cr and Ni, two carbon steels of semi-killed steel SM41 and killed steel S35C, two aluminum materials of 1200 aluminum and 5083 alloy which contained 4.5 % Mg and additionally TP28 titanium. All of these materials were rolled except the cast steel of 30Cr-16NiN, then prepared as a board shape of 200 to 300 mm in length, 100 mm in width and 30 mm in thickness.

2.2 Welding Equipment and Welding Conditions

150 KV-40 mA Hamilton type EB-welder was

Table 1. Chemical composition of material used.

Element / Material	wt (%) C	Si	Mn	P	S	Fe	Ni	Cr	Cu	Al	Mg	Zn	Ti	ppm H	O	N
SUS 27	0.08	0.79	0.99	0.025	0.010	Bal.	8.76	18.29						4.4	29	230
SUS 27N	0.02	0.45	1.53	0.006	0.009	Bal.	10.10	18.70						2.5	99	1950
30Cr-16NiN	0.25	0.83	1.30	0.020	0.010	Bal.	16.15	30.56						7.0	75	2325
SM 41	0.18	0.04	0.79	0.090	0.150	Bal.								0.0	316	35
S 35C	0.33	0.25	0.74	0.160	0.170	Bal.								0.1	6	35
1200		0.13	0.01			0.540			0.030	Bal.		0.010		0.4	24	16
5083		0.14	0.64			0.210		0.15	0.040	Bal.	4.60	0.010	0.020	0.4	6	16
TP 28	0.006					0.053							Bal.	21.0	700	50

† Received on Nov. 25, 1972

* Professor

** Kawasaki Heavy Industries, Ltd.

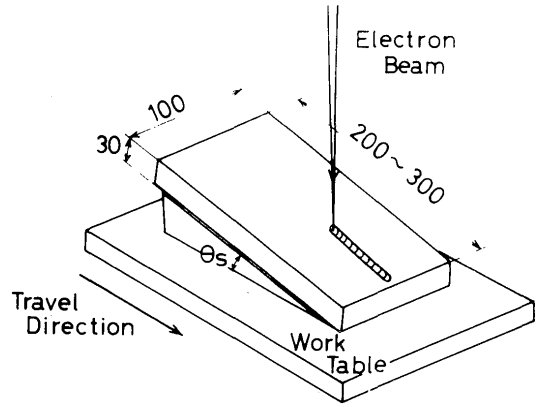

Fig. 1. Slope-welding employed in this experiment.

employed to make the welding bead on these specimens. The experimental method of slope welding was employed as shown in **Fig. 1.** The welding bead was made on the workpiece fixed on a moval table traveling horizontally, and it is set at a certain slope angle, $\pm\theta_s$, with respect to the horizontal plane, crossing at right angle with the beam axis. We call "upslope welding" for $+\theta_s$ slope and "downslope welding" for $-\theta_s$ slope, and it has been done at $\pm 30°$ in this experiment.

Defining as given in **Fig. 2** various kinds of welding parameter the beam active parameter(active parameter), $a_b(\equiv D_O/D_F$, D_O: object distance, D_F: focal length), becomes the most important once, and its value is changed continuously by using slope welding mentioned above as show in **Fig. 2.** In this experiment, as the visual beam active parameter a_b^* was

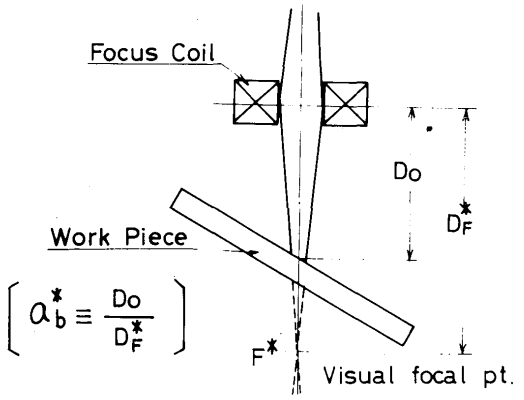

Fig. 2. Schematic explanation of D_O, D_F^* and a_b^*.

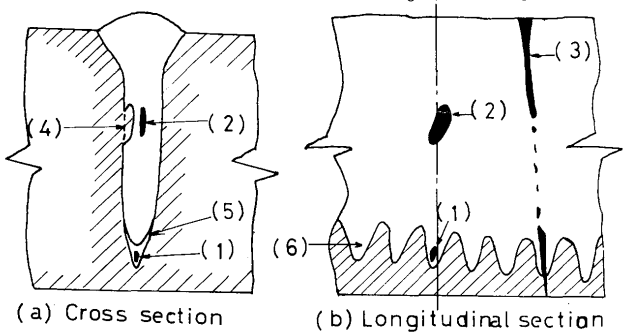

Fig. 3. Schematic illustration of various macroscopical beam weld defects. (1) R-Porosity, (2) A-porosity, (3) AR-Porosity, (4) Unmelted lump, (5) Cold Shut and (6) Spiking

used, where $a_b^* \equiv D_O/D_F^*$ (D_F^* is visual focal length and defined as the distance between the center of the focusing lens and the visual focal spot which is observed visually as the smallest brilliant point on the surface of workpiece, with so small current that unable to melt it), and its value was the range from 0.46 to 0.93 at $D_F^*=280$ mm.

The welding was mainly performed under following conditions: $V_b=150$ KV (beam voltage), $I_b=10 \sim 40$ mA (beam current), $v_b=30 \sim 240$ c. p. m. (welding speed), $P_{ch}=4\times10^{-4}$ Torr (pressure of work chamber), $D_F^*=280$ mm and $\theta_s=\pm30°$.

3. Experimental Results

3.1 Classification of Weld Defects except Cracks

The weld defects observed in longitudinal and transversed cross-section of the specimens are basically classified as shown in **Fig. 3.**

(1) R-Porosity (Root Porosity)

This porosity occurs at the tip of the penetration depth,[1] that is, the vicinity of the root and tends to occur the more at the deeper zone of the penetration. **Photo. 1** and **Photo. 2** show the macro structure in the transverse section and the longitudinal section respectively. Especially in **Photo. 2,** the distribution of the R-porosity is observed at a glance.

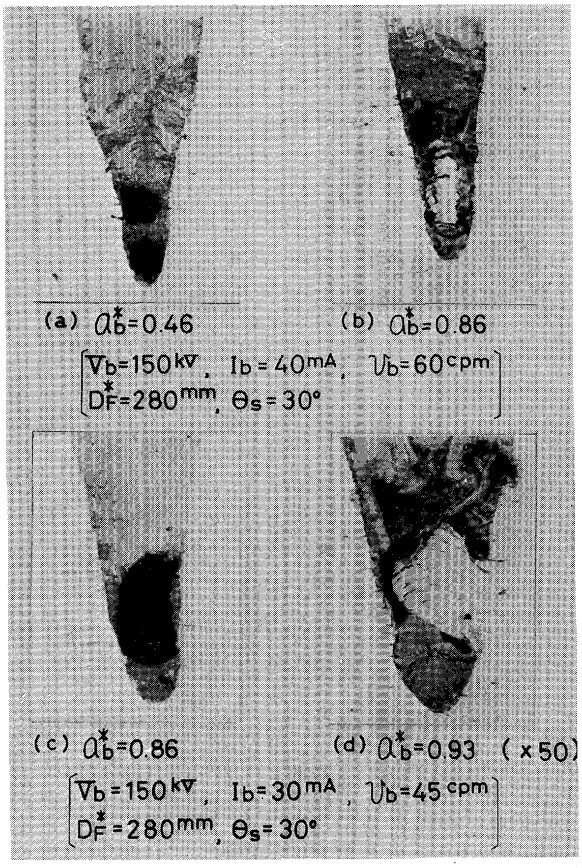

Photo. 1. R-porosity and unmelted lump in the cross-section of SUS27 beam weld.

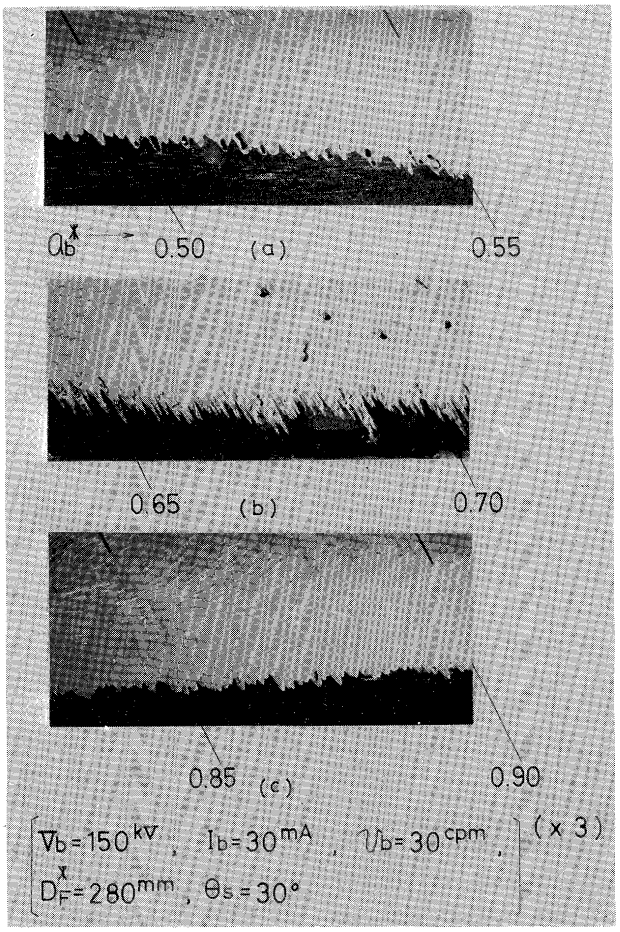

Photo. 2. Spiking, R and A-porosity in the longitudinal-section of SUS27 beam welds.

(2) A-Porosity (Active Zone Porosity)

This porosity occurs due to the violent action of the active zone of the beam and appears in the vicinity of the travelling path of the beam active zone which makes a bead width minimum or so. **Photo. 3** and **Photo. 2 (b)** show its macro-structures in the transverse section and the longitudinal section.

Especially **Photo. 2 (b)** is indicated precisely the distribution of the A-porosity. This porosity was recognized to occur in stainless steel and carbon steel, but not in aluminum and titanium under this experimental condition.

(3) AR-Porosity (Arcing Porosity)

As shown in **Photo. 4** authors recognized a long porosity which was composed of a chain porosity in the longitudinal section, which connects up usually to the bead surface

This porosity occurs due to the arcing in the electron gun. Such arcing occurs mainly due to the weld vapours generating violently during welding, and in general it tends to occur severely in aluminum and titanium compared with stainless steel and carbon steel. Moreover it is recognized that the AR-porosity usually brings about the formation of needle-like spiking with the R-porosity.

(4) Unmelted Lump

As shown in **Photo. 1 (b), (d)** and **Photo. 3 (b),** unmelted zone either connected or disconected with the parent metal, "unmelted lump", was observed

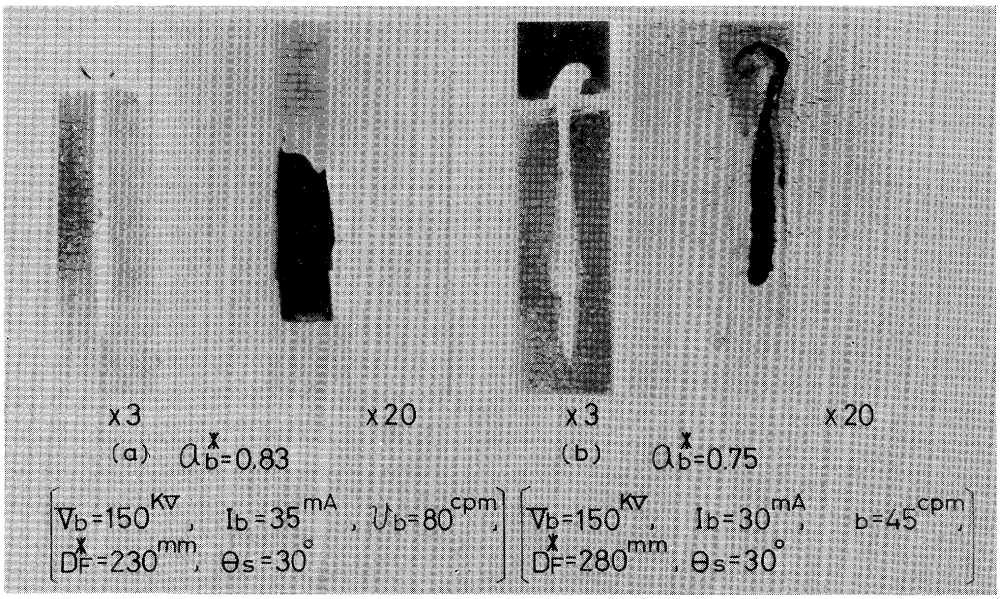

Photo. 3. A-porosity and unmelted lump in the cross-section of SUS27 beam welds.

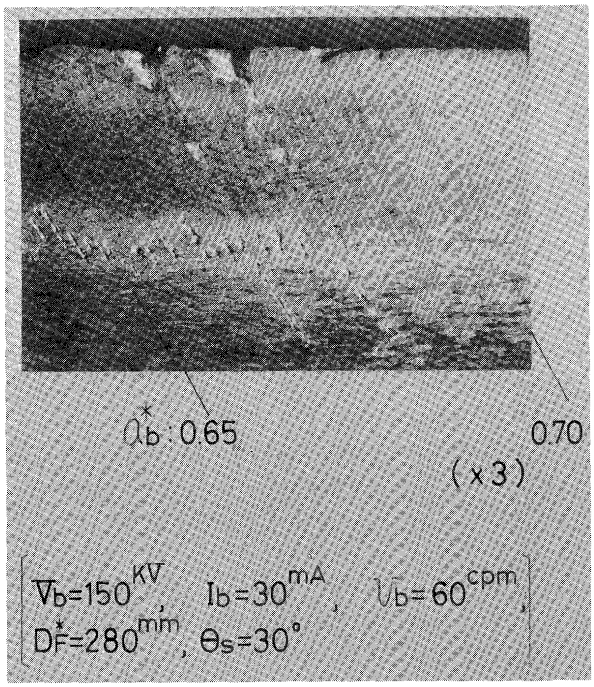

Poto. 4. R and AR-porosity in the longitudinal-section of 1200 beam welds.

inside the weld deposite. Usually it has a tendency to be co-existence with R or A-porosity.

(5) Cold Shut

It is well known that this defect is often found in the electron beam welds[2] and especially near the root zone as shown in **Photo. 5.**

(6) Spiking

The spiking-like penetration, "spiking", is indicated in **Photo. 2** adopted the longitudinal section of welds. As it is well known,[3] it is peculiar phenomenon generating in the high energy density beam welding such as the electron beam welding and is recognized

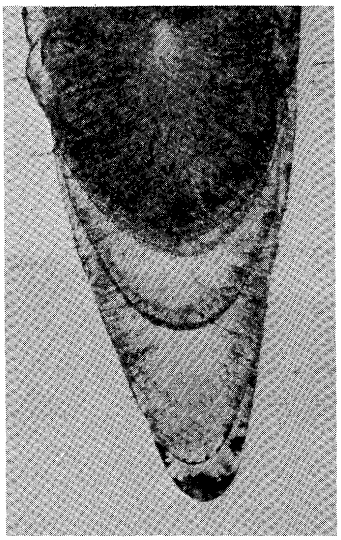

Photo. 5. Cold shut in the cross-section of SUS27 beam welds.

to occur in all materials used. Some of them present strong featurs, others weak ones, and also needle like spiking often appears, especially near the existence region of the former. We call strong spiking, weak spiking and needle spiking respectively. The strong spiking or needle spiking will be taken occasionally as a weld defect.

3.2 Characteristics of R and A-Porosities

The effect on the occurring of A and R-porosity of the welding procedure, materials and so on, was examined and discussed.

3.2.1 Effect of Welding Procedure

The experiment was performed under the same welding conditions as described in chapter **2.2** using the four materials (SUS27, SM41, 1200 and TP28). Typical results obtained are shown in **Fig. 4 (a)～(d).**

To examine the occurring zone of the porosity, weld bead appearance, radiograph and macro-structure of longitudinal section are observed, and its zone was indicated using beam active parameter, a_b^*.

One of these examples is shown in **Photo. 6.** From these results, the occurrence of A and R-porosity are recognized in SUS27 and SM41, while only R-porosity occurs but A-porosity doesn't ocuur in 1200 and TP28 under our experimental condition. The occurence of porosity is shown in **Fig. 5** used an indication, Δa_b^* (a_{b1}^*- a_{b2}^*) which expresses the existence range of the defects: "defect range" From this figure, it is understood that the defect range, Δa_b^* of A-porosity is fairly proportional to beam current, but that of R-porosity show different feature in each materials.

And using the EB-weldability based on the defect range of porosity, TP28 is the best, as the order of 1200, SUS27 and SM41. So, SM41 is worst among these materials.

The effect on the occurring zone of the focal distance, D_F^* and the slope angle, θ_s in the slope-welding was examined for SUS27. Using D_F^* at 180, 280 and 380 mm, obtained results are shown in **Fig. 6 (a)** and **(b).** In case of upslope welding (θ_s=30°) and downslope (−30°) obtained results are shown in **Fig. 7** and **Fig. 8,** also the radiographs of both case are shown in **Photo. 7.** Then it is recognized that the occurring zone of R-porosity in the both case have a little difference but that of A-porosity have the distinguished difference.

This phenomena is also recognized in SM41.

3.2.2 Effect of Material

The porosity diagram as shown in **Fig. 4 (a), Fig. 9** and **Fig. 10,** was obtained about three types of austenitic stainless steel specimens. In this case, the

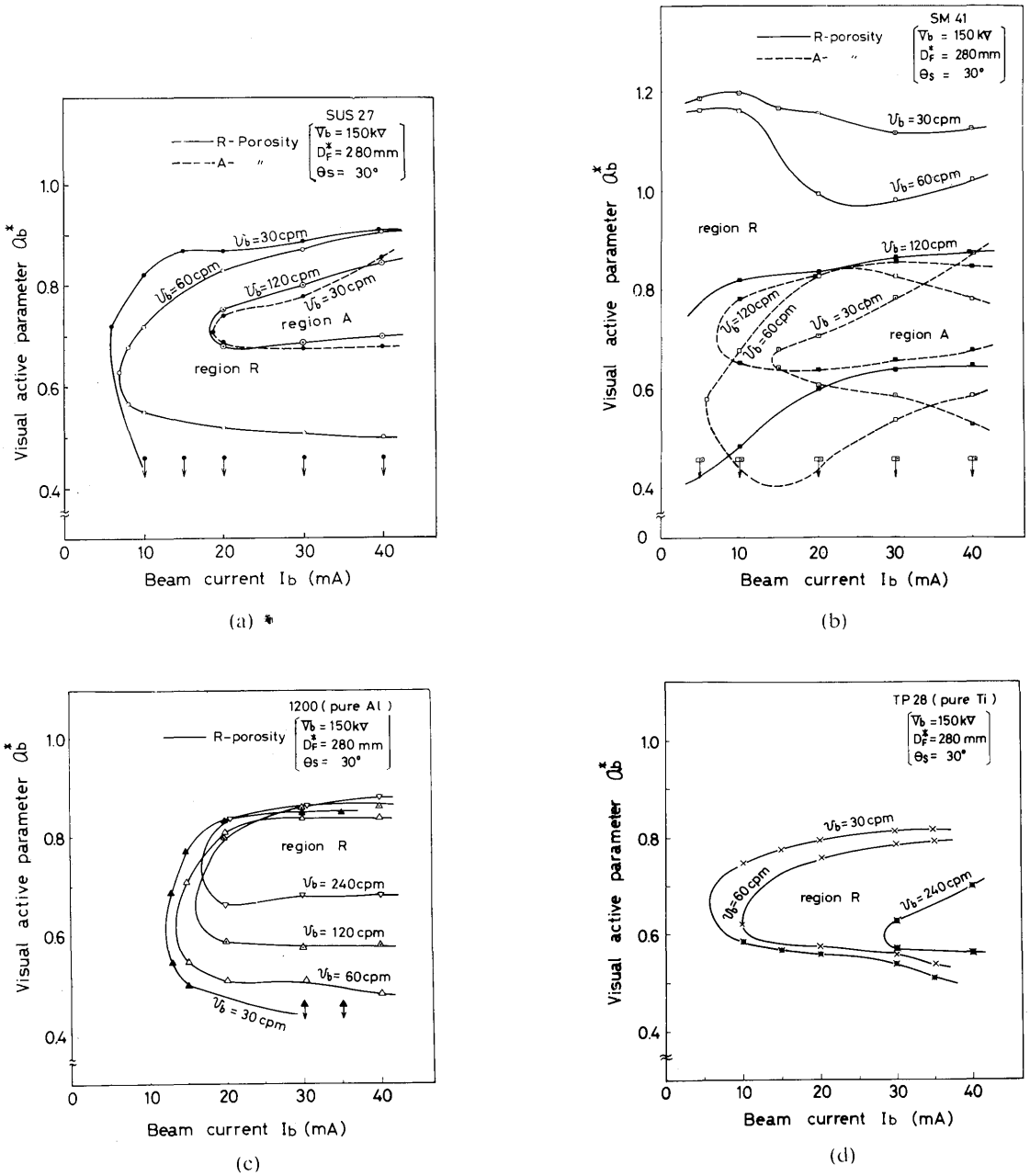

Fig. 4. Porosity diagrams of beam welds. (a) SUS27, (b) SM41, (c) 1200 and (d) TP28.

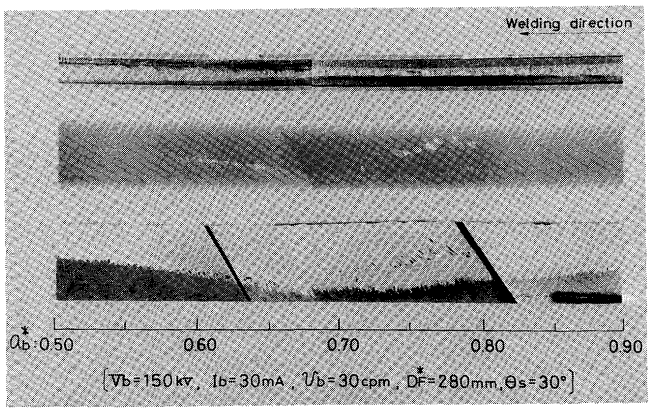

Photo. 6. Bead appearance (top side), radiograph (middle) and longitudinal-section (bottom side) of SUS27 beam welds.

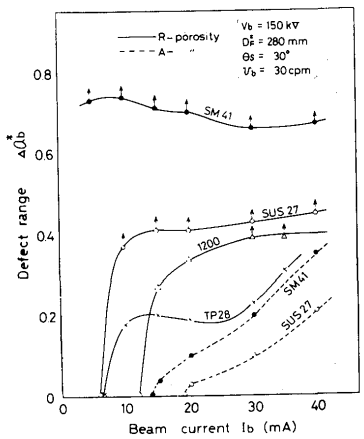

Fig. 5. Porosity diagram indicated relation between beam current and defect range in typical used specimens.

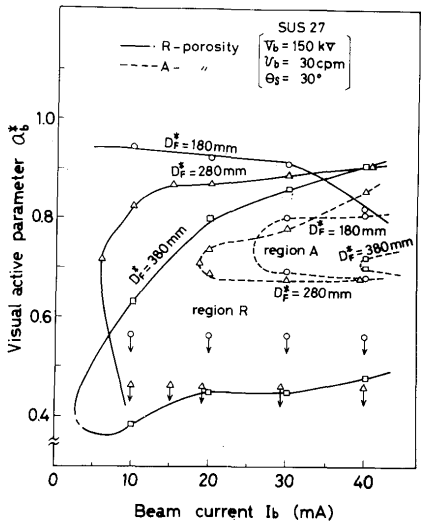

(a)

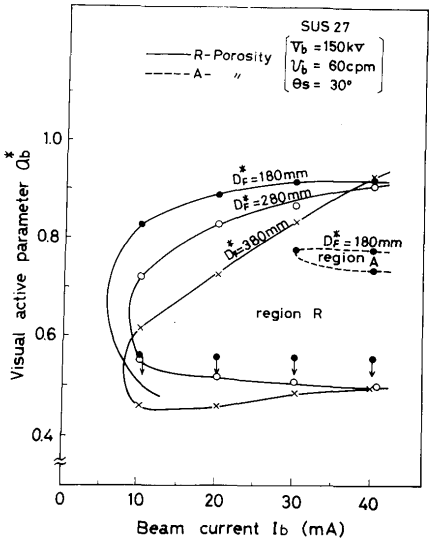

(b)

Fig. 6. Effect of focal length.
(a) v_b=30 c. p. m. and (b) v_b=60 c. p. m.

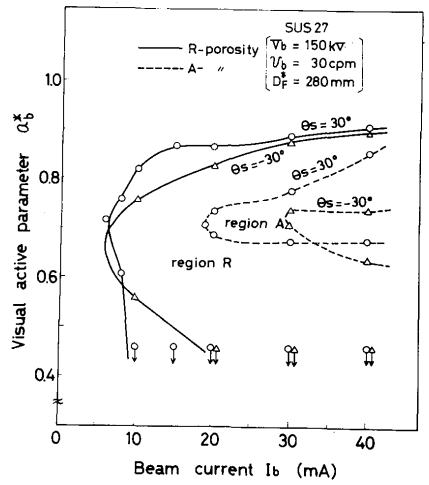

Fig. 7. Porosity diagram indicated effect of upslope and downslope-welding. (SUS27)

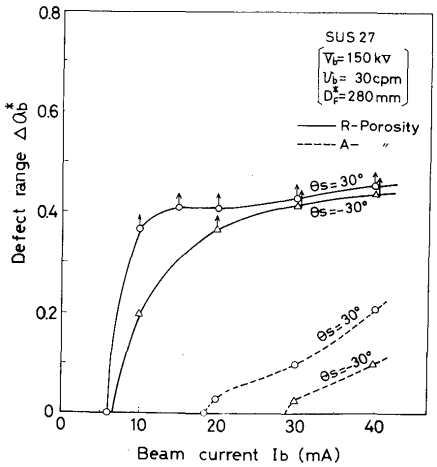

Fig. 8. Porosity diagram indicated effect on defect range of upslope and downslope-welding. (SUS27)

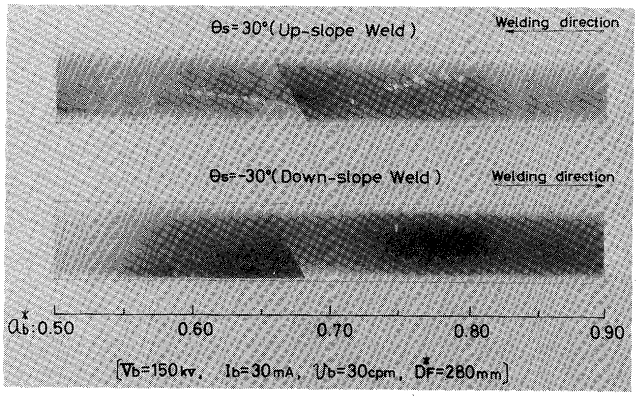

Photo. 7. Radiographs of upslope and downslope beam welds of SUS27.

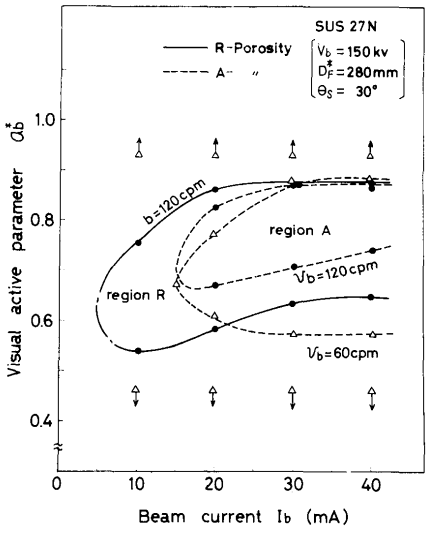

Fig. 9. Porosity diagram in SUS27N beam welds.

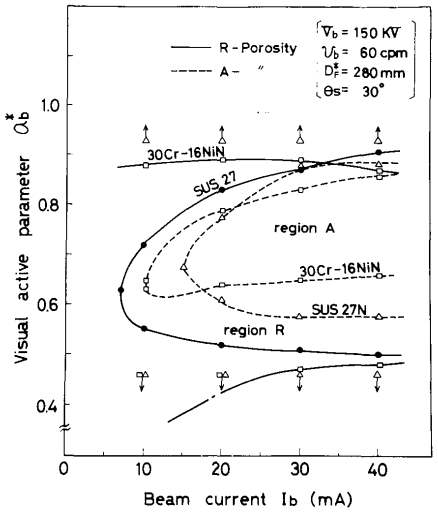

Fig. 10. Porosity diagram of austenitic stainless steels.

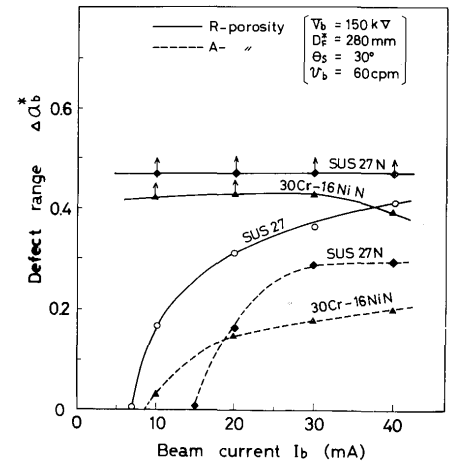

Fig. 11. Porosity diagram indicated relation between beam current and defect range in the austenitic stainless steel.

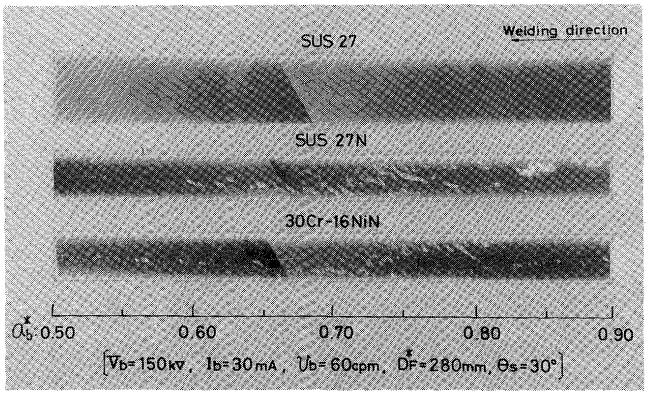

Photo. 8. Radiographs of upslope beam welds of SUS27, 27N and 30Cr-16NiN.

defect range, Δa_b^* and radiograph of the welds were shown in **Fig. 11** and **Photo. 8** respectively.

In these materials, it was proved that nitrogen gas contained fairly controlled the occurrence of porosity,

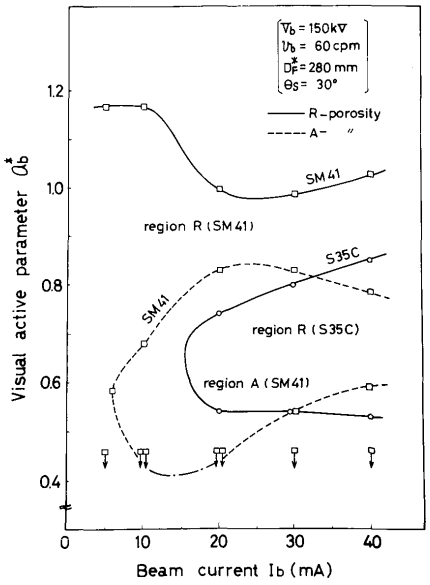

Fig. 12. Porosity diagram of SM41 and S35C.

and that its occurring range increased with increasing nitrogen content. The porosity diagram of SM41, S35C carbon steel is shown **Fig. 12** using 60 c. p. m. welding speed.

Thus, it was recognized that the porosity range in the carbon steel remarkably was increased by oxygen same as nitrogen in austenitic stainless steels.

In general, the penetration depth of 5083 alloy[5] is deeper considerably compared with that of 1200 aluminum and needle-like R-porosity occurs remarkably, but A-porosity doesn't occur as shown in **Photo. 10.** However, liny AR-porosity sometimes occurs through the location corresponding to R and A-porosity region considered as shown in **Photo. 9.**

With increasing the beam current, arcing tends to occur easily and AR-porosity is caused, and when the arcing continues generating of the beam becomes impossible. Compared with the oxygen gas content of 1200 aluminum, TP28 titanium contains extremely high,

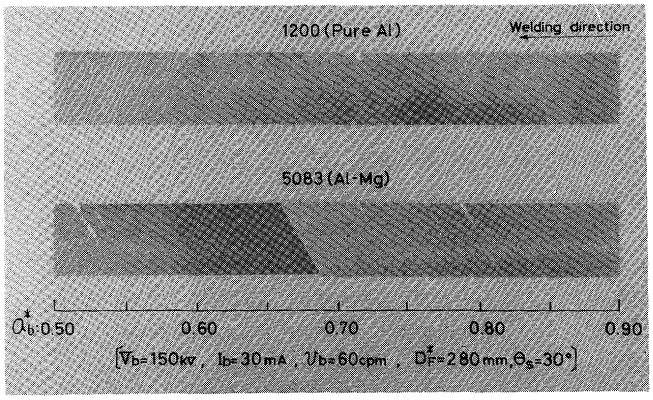

Photo. 9. Radiographs of upslope beam welds of 1200 and 5083.

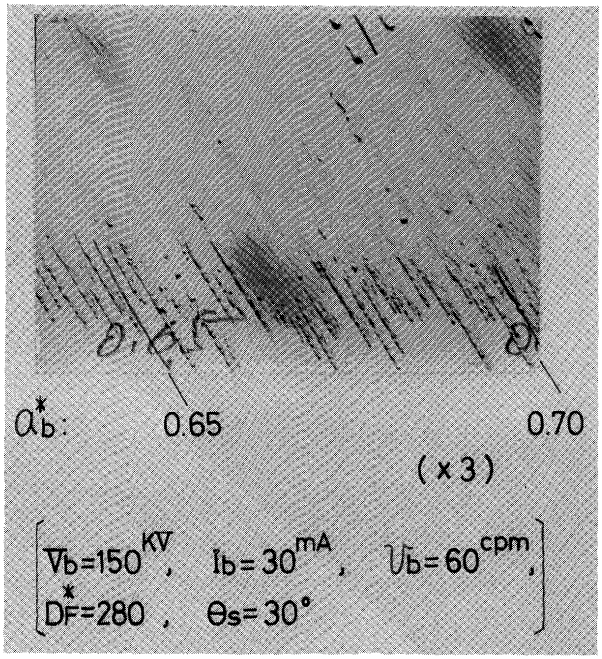

Photo. 10. R-porosity in the longitudinal-section of 5083 beam welds.

neverthless, R-porosity range is small, and A-porosity does not occur. It seems that titanium prevents the occurrence of porosity due to the oxygen.

3.2.3 Some Discussions

The relation between penetration depth and numbers of R-porosity and spike is shown in **Fig. 13 (a), (b)** and **(c).** Moreover these figures contain the both results of upslope welding (θ_s=30°) and downslope welding (θ_s=−30°).

Then it seems that the occurrence of R-porosity has no connection directly with the depth of the penetration but is crosely connected with the spiking, because each maximum point of numbers of R-porosity, N_p, and numbers of spikes, N_s, agrees with each other around a_b^*=0.65 (θ_s=30°) or a_b^*=0.55 (θ_s =−30°) without regard to the materials and welding procedure, such as upslope or downslope but that of penetration depth, h_p, and N_p doesn't in case of downslope (θ_s=−30°).

Provided that symbol A_a represents sum of the area of A-porosity located at given a_b^* -point in the longitudinal section, **Fig. 14 (a), (b)** indicates the relation between A_a, h_p and bead width, d_B, and both of the maximum point of A_a and minimum point of d_B agree with each other around a_b^*=0.70∼0.75 without regard to the materials and welding procedure such as upslope or downslope. Then it seems that the formation of A-porosity has no connection directly with maximum depth of the penetration, but is closely connected with the region of the minimum bead width.

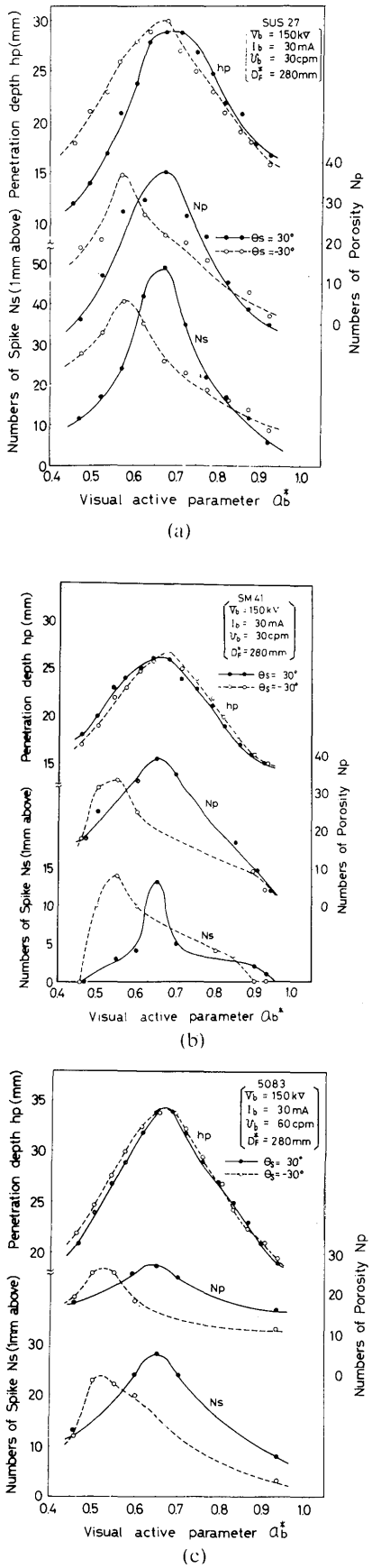

Fig. 13. Relation between penetration depth and both numbers of R-porosity and spike.
(a) SUS27, (b) SM41 and (c) 5083.

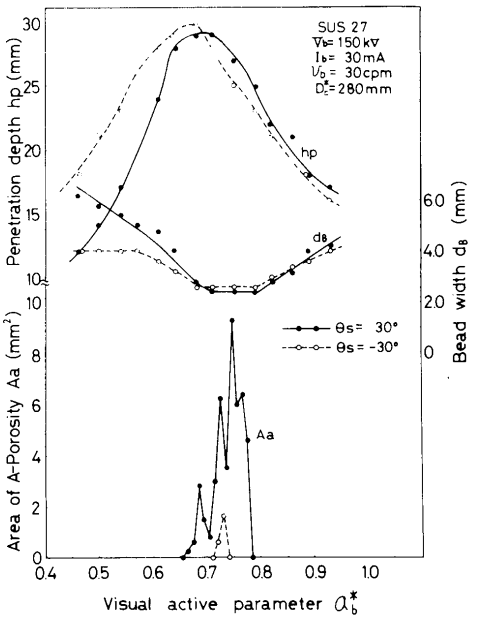

(a)

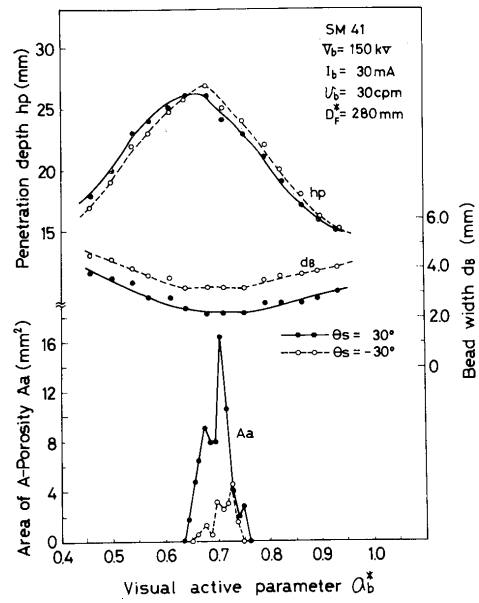

(b)

Fig. 14. Relation between area of A-porosity, bead width and penetration depth.
(a) SUS27 and (b) SM41

In the slope-welding in general, the mutual relation on situations between shape of the beam, specimen and shape of the penetration is given as shown in **Fig. 15.**[4]

The location of the porosity in this schematic explanation was obtained from **Fig. 15,** and moreover the shape of the bead obtained due to the upslope-welding was employed in stead of the shape of the actual beam, because both of them fairly with each other.

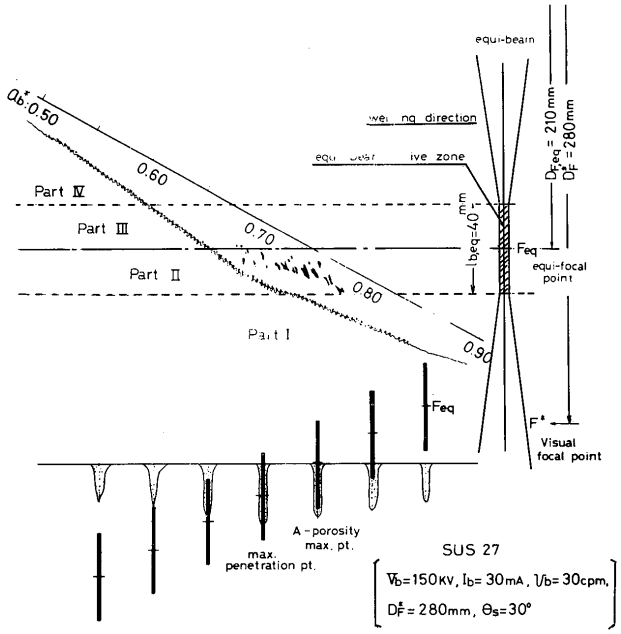

Fig. 15. Schematic explanation of mutual relation on situations between occurring range of porosity and equi-beam.

Then we call such slope-weld bead shape "equivalent beam" or "equi-beam" whose profile is obtained projecting such slope bead at the location of the actual beam.

The mutual relation on the situation between equi-beam and specimen is considered in four parts, I~IV in **Fig. 15.** The difference of the characteristics of porosity occurrence in each section are recognized as follows:

(1) Part I: welding is performed using the upperfocus beam whose energy density is relatively low, and the beam active zone has no action there. In this region, only R-porosity tends to occur and its shape of penetration is well type as shown in **Photo. 11 (b).**

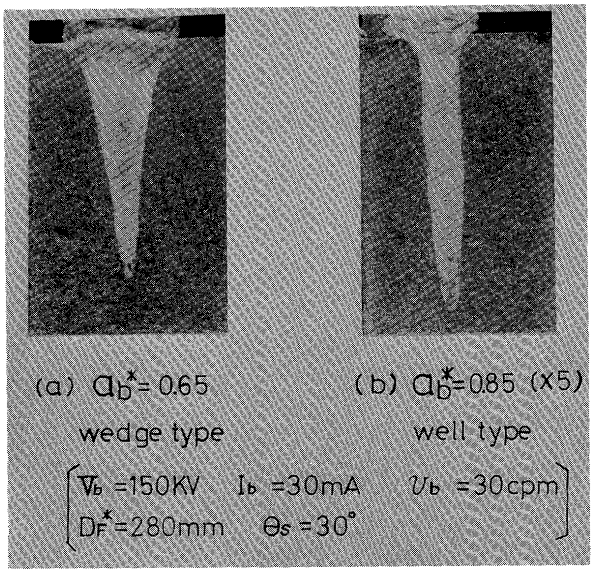

Photo. 11. Sectional profile the bead penetration of 1200.

(2) Part II: lower part, l_{b2}, of the beam active zone with the strong energy density. In this region, the occurrence of A-Porosity are the most. Especially around the just focus, $a_b=1$ or $a_b{}^*=0.75$, it occurs violently and much R-porosity occur also. In this region, the penetration depth becomes the deepest around $a_b{}^*=0.70$.

(3) Part III: The surface of the specimen is exposed to the upper part, l_{b1}, of the beam active zone. In this region, R-porosity occurs so much, but A-porosity occurs very few, and the penetration depth gradually decreases with being apart from Part II and its shape tends to wedge type.

(4) Part IV: welding is performed using the under-focus beam whose energy density is as low as in Part I and its beam active zone is no concern there. In this region, only R-porosity tends to occur and the penetration depth decreases still more than in Part III.

4. Conclusion

Kind of macroscopic beam weld defects (except crack) and occurring characteristics of R, A and AR-porosity have been investigated using slope-welding.

Obtained results are as follows:

(1) R-porosity, A-porosity, AR-porosity, unmelted lump, cold shut and spiking as macroscopic defects in the beam welds have been observed.

(2) In electron beam weld of Austenitic stainless steel and carbon steel, occurring of porosity was remarkably affected by content of Nitrogen and Oxygen in these materials, and as these contents increase, occurring range of A and R-porosity increase.

(3) In electron beam welding of Aluminum alloys contained such high vapour pressure element as Magnesium, both of the occurring zone of R-porosity and the penetration depth remarkably increases in comparison to pure Aluminum and the porosity shape becomes like a needle. Although A-porosity does not occur, AR-porosity tends to occur there.

(4) Occurring of R-porosity directly is no concern with penetration depth but closely concern with spiking.

(5) Occurring of A-porosity is closely concern with both of the location and shape (length, diameter and profile) of the beam active zone, beam power and its density.

(6) Porosity diagram which is indicated using parameters of $a_b{}^*$, $\Delta a_b{}^*$, l_b and so on, can be sufficiently utilized in a electron beam welding and also it can be employed to search useful welding condition to protect porosity occurrence.

References

1) Meleka: "Electron-beam Welding", Published by Mcgraw-Hill (1971).

2) F. Matsuda, T. Hashimoto and Y. Arata: "Some Metallurgical Investigations on Electron-beam welds", Trans. Japan Welding Society, Vol. 1 No. 1 72-85 (1970).

3) R. E. Armstrong: "Control of Spiking in Partial Penetration Electron Beam Welds" Welding Journal, Vol. 50 No. 8 (1970).

4) Y. Arata: "Characteristics of the Electron Beam Heat Source and View of the Development on its Welding Technology", J. Japan Welding Society, Vol. 41, No. 11 (1972).

5) M. Ohosumi: Lecture in EBW Comittee of Japan Welding Society, Society, (1971).